NASA - X-614-63-210

OTS: $3.60 ph; $1.22 mf

N64 11799

CODE-1

(NASA TMX-51258;

[1963] 34 p refs

SCIENTIFIC RESULTS OF OSO-1

BY

JOHN C. LINDSAY

Conf.

OTS PRICE

XEROX $ 3.60 ph

MICROFILM $ 1.22 mf

Corp author: NASA

GODDARD SPACE FLIGHT CENTER

GREENBELT, MD.

(Presented at AIAA/CASI/RAeS 9th ANGLO-AMERICAN CONFERENCE, October 16-18, 1963)

SOT-10832

SCIENTIFIC RESULTS OF OSO-1

THE OSO-1 SPACECRAFT

A new era in the study of the sun from above the earth's atmosphere began with the successful launching of the first Orbiting Solar Observatory on March 7, 1962. Prior to this launch, measurements of solar radiations that are absorbed in the atmosphere had been made from balloons, rockets, and rather simple earth satellites. As a result of the various restrictions imposed by these techniques it was not possible to achieve a reasonable degree of observation continuity such as has now been accomplished by the OSO-1. The characteristics of the spacecraft that made this performance possible were the ability of the spacecraft to point instruments accurately at the sun, a circular orbit of approximately 575 km altitude below most of the radiation belt but above the atmosphere, and a tape recorder data storage system that supplied complete orbit coverage.

The OSO-1, like many other satellites, used the gyroscopic properties of a spinning body for stability. However, unlike other spacecraft, an integral part of OSO-1 was a unique biaxial attitude control system to point instruments at the center of the sun. The spacecraft, Figure 1, (Dolder, Bartoe, Mercure, Gablehouse and Lindsay [1]) consisted of two parts, a wheel section and a platform upon which the solar cell array was mounted. The wheel section was spun to provide spacecraft stability, the spin axis being maintained approximately perpendicular to the solar vector with cold gas precession jets. Driving against the wheel section,

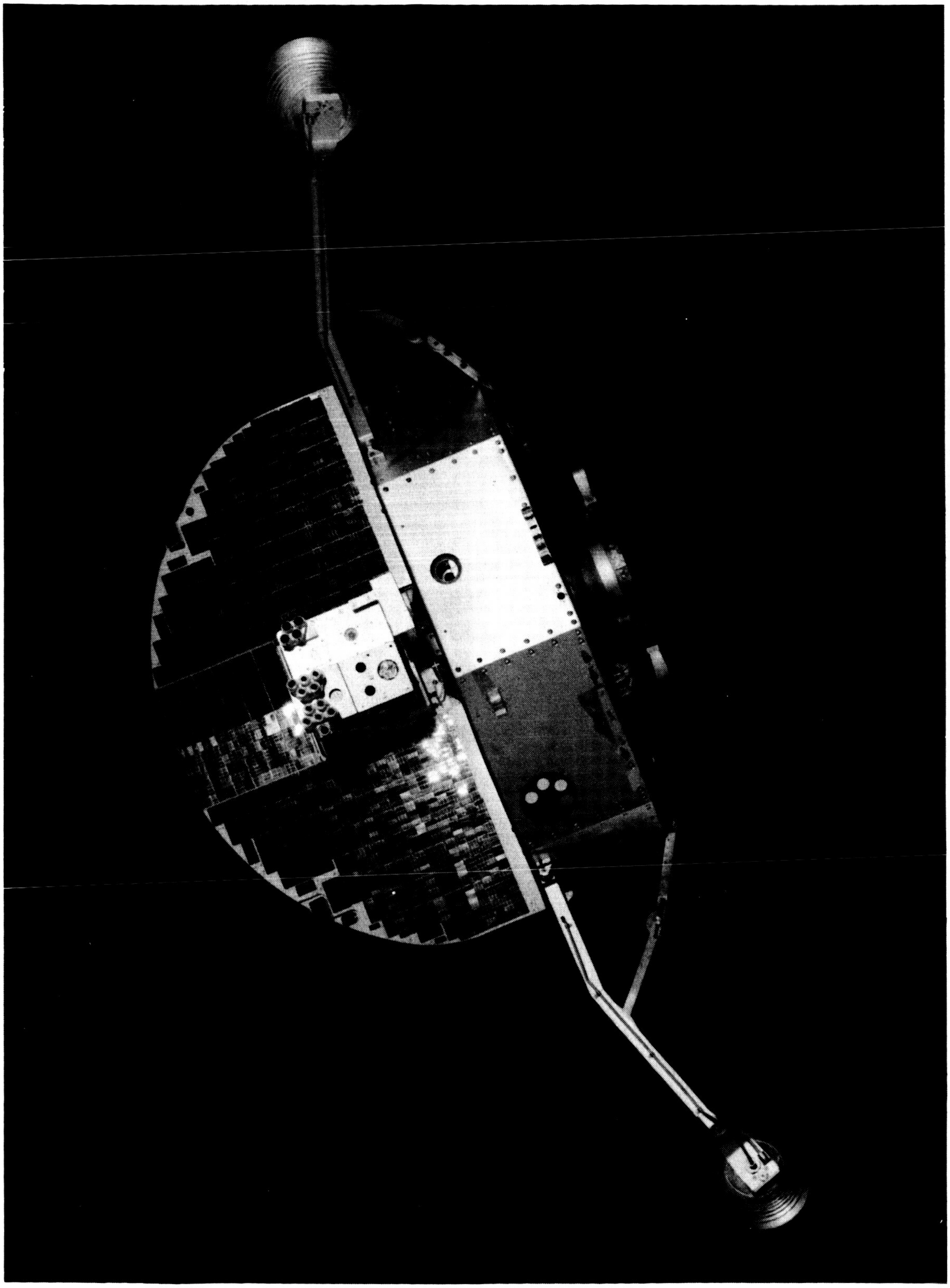

Figure 1 - OSO-1 Spacecraft

an electrical servo-system oriented the platform perpendicular to the solar vector around the spin or azimuth axis. A second servo-system within the platform oriented an instrumentation section toward the sun in elevation. In this manner, the pointed instrumentation section was oriented along the solar vector in two axes. The spin of the wheel system was maintained by a gas system mounted on the end of arms.

A total of over a year's operation was obtained from the satellite with near perfect performance for approximately three months and real-time data recovery for a period of about nine months. Although there were some problems with the pointing system during the life of the satellite, the long term pointing accuracy was within approximately two minutes of arc in both azimuth and elevation.

One might summarize the engineering firsts of OSO-1 as follows:

1. The first of the observatory spacecrafts, with demonstrated solar pointing more accurate than previously obtained with satellite or rocket systems.
2. First long-time operation of D.C. torque motors, bearings, slip rings and other moving parts in the space environment for an extended period of time, 18 months. An example of slip ring performance is shown in Figure 2.
3. A unique damper to minimize spacecraft wobble.
4. First scientific spacecraft utilizing tape recorders to obtain complete orbit data coverage.

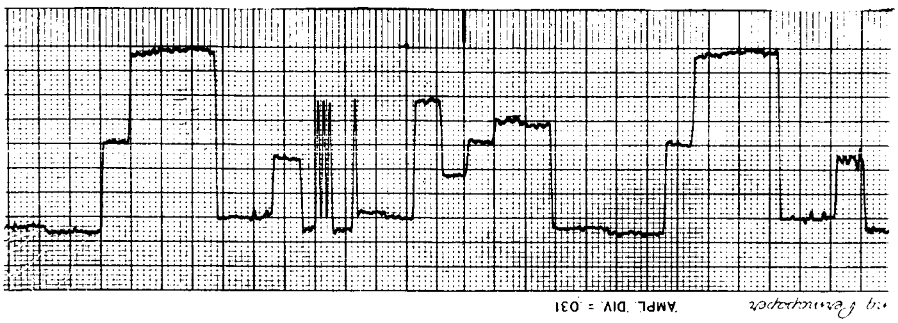

ORBIT 1708

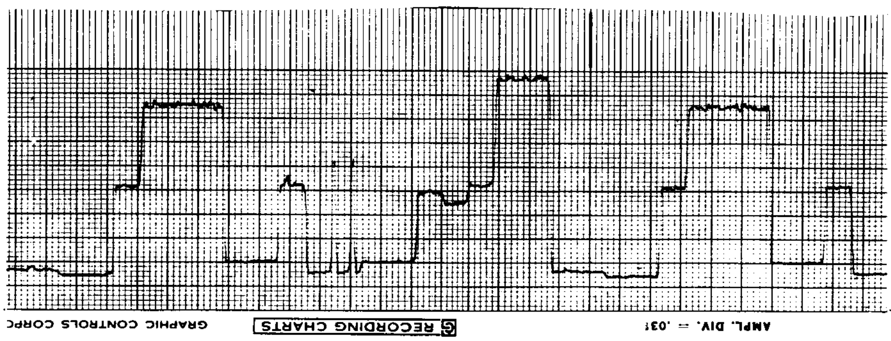

OR BIT 5004

S-16 Goddard Pointed Experiment Data

Figure 2 - Slip Ring Performance (Data shown for Orbits 1708 and 5004 were transmitted through slip rings from sail to wheel section of the satellite)

THE OSO-1 SCIENTIFIC EXPERIMENTS

1. Extreme UV Spectrometer

The primary solar oriented experiment aboard OSO-1 was a scanning spectrometer used for observation of the solar extreme UV radiation from 50-400 A (Behring, Neupert and Lindsay [2]).

During operation the spectrometer was pointed at the center of the solar disk within approximately two min of arc. In this orientation, radiation from the entire solar disk and inner corona passed directly through the entrance slit and struck a concave grating mounted in grazing incidence, the angle of incidence being 88^{o}. The grating, an original ruled in a special glass by the Nobel Institute in Stockholm, had 576 lines per millimeter on a blank of one meter radius of curvature. The exit slit and detector were mounted on a carriage which was driven on a circular rail so that the exit slit scanned along the Rowland Circle, where the spectrum was focused, from 10-400 A. The plane of the exit slit was approximately perpendicular to the diffracted ray at all positions along the track, thereby keeping the spectral passband nearly constant for all angles of diffraction. The 50 micron entrance and exit slits provided a spectral passband of 1.7 A and permitted resolution of lines 0.85 A apart. The detector was a windowless photomultiplier developed by the Bendix Corporation specifically for use in this spectrometer. A tungsten photocathode was chosen to minimize response to wavelengths above 1500 A, and to reduce changes in sensitivity due to variations of the emission properties of the cathode.

The spectrum obtained from the spectrometer over wavelengths of 170 A to 400 A is shown in Figure 3. The brightest emission line in the region from 170 A to 340 A is the Lyman-alpha line of ionized helium at 304 A. In addition, numerous other emission lines appear with combined flux comparable to, or somewhat greater than, that of the helium line. Resonance lines of heavy ions (Mg through Fe) are expected in this region, leading to attempts (Zirin, Hall and Hinteregger [3]), (Neupert and Behring [4]), to identify the more prominent features of the spectrum in terms of such lines. Other than the 304 A line of He II Lyman-alpha, the only lines identified with relative certainty are the 284 A line of Fe XV and the 335 A line of Fe XVI.

The months of March and April of 1962, were ideal for a study of the solar EUV spectra (Neupert, Behring and Lindsay [5]) in that observations could be made on both a quiescent and a disturbed solar atmosphere. During the second week in March the sun was especially quiet, the sunspot number being zero on 11 March. As the month progressed the solar rotation carried several centers of activity across the visible hemisphere of the sun. Definite enhancements in the solar spectrum were associated with these centers of activity.

Figure 4 presents two scans of the EUV spectrum which were obtained with a separation in time of approximately ten days. During the first of these observations only one small region of activity was present on the solar disk. In spite of this low level of activity it is observed that the Fe XV and Fe XVI lines persist as two of the more prominent

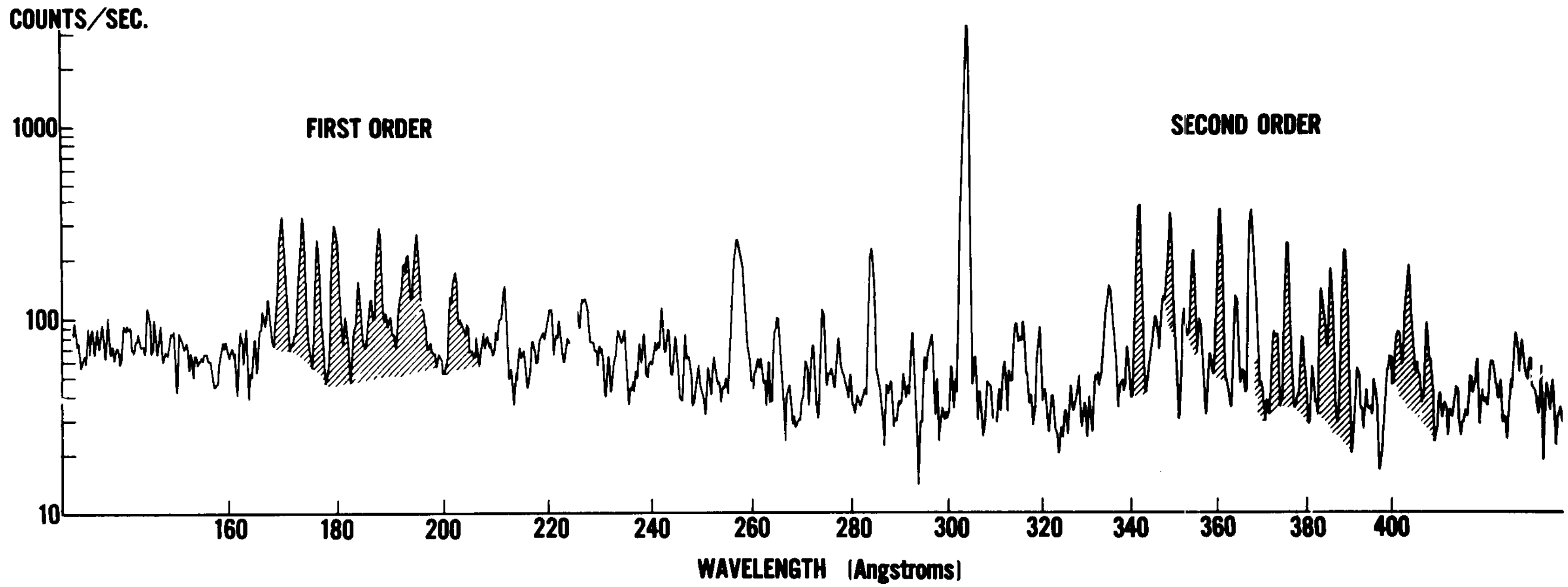

Figure 3 - Typical Solar Spectrum 170 A - 400 A

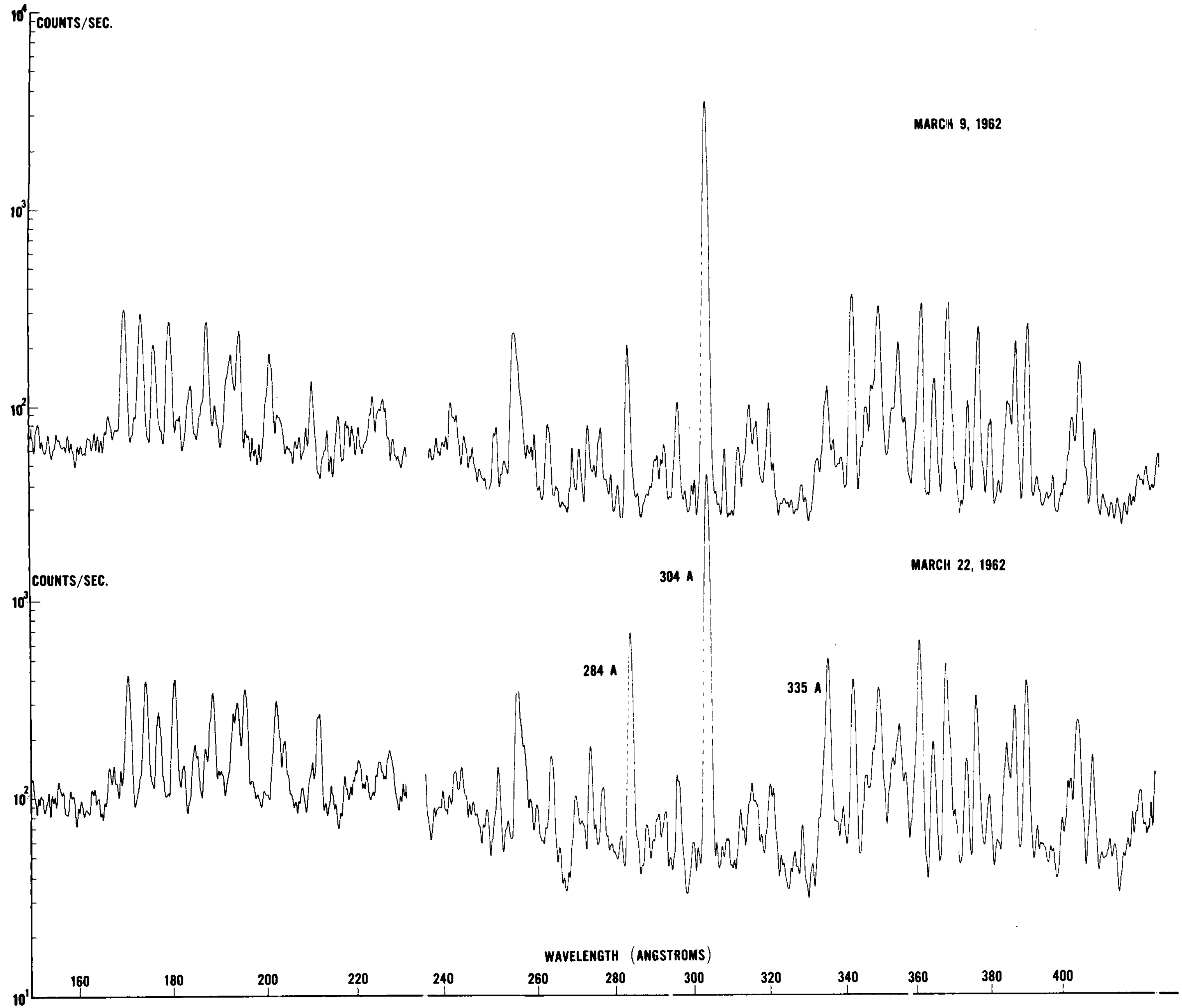

Figure 4 - Comparison of Two Spectra Representing "Quiet" and "Active" Sun

features of the spectrum. The second spectrum was obtained while several large and well-developed centers of activity were present on the disk. Comparing these two spectra we observe that the emission lines have increased in intensity but not all by the same amount. The Fe XV and Fe XVI lines, already prominent even in the absence of solar activity, have increased in intensity appreciably more than any other line observed with certainty in this spectral range. The He II line has also increased, but by a lesser amount.

The relationship of these observed counting rates to several ground-based measurements of solar activity is presented in Figures 5 and 6. In Figure 5, the He II radiation is compared with daily values of the solar flux at 2800 Mc, and with the Zurich Provisional Relative Sunspot Number (ZPRSN). Also shown is an estimate of the calcium plage area, each area being weighted by the estimated intensity of the area on a scale from 1 to 5. Values for this computation were supplied by the McMath-Hulbert Observatory. In Figure 6, the daily values of solar flux at 2800 Mc and the Zurich Provisional Relative Sunspot Number are compared with radiation due to the coronal lines of Fe XV (284 A) and Fe XVI (335 A). The estimated calcium plage intensity is also shown.

The spectral lines chosen for presentation here were selected because they are reliably identified with particular ions, not because they convey more than any other line in the spectrum the changes in solar flux which occur with the appearance of plage areas. In terms of fractional changes in intensity, these three lines represent the extremes which have

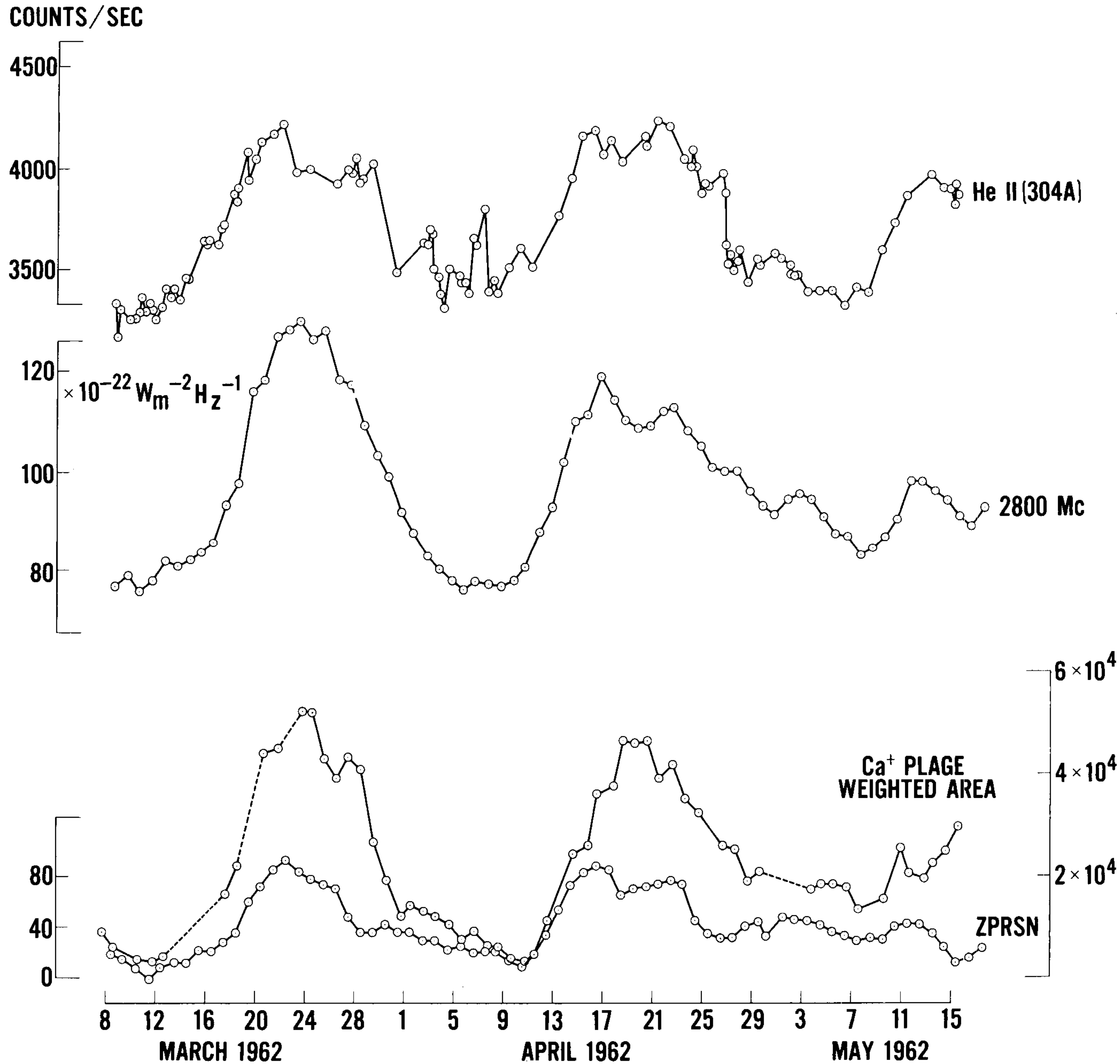

Figure 5 - He II Lyman-alpha Line Compared with Ground-based Measurements of Solar Activity

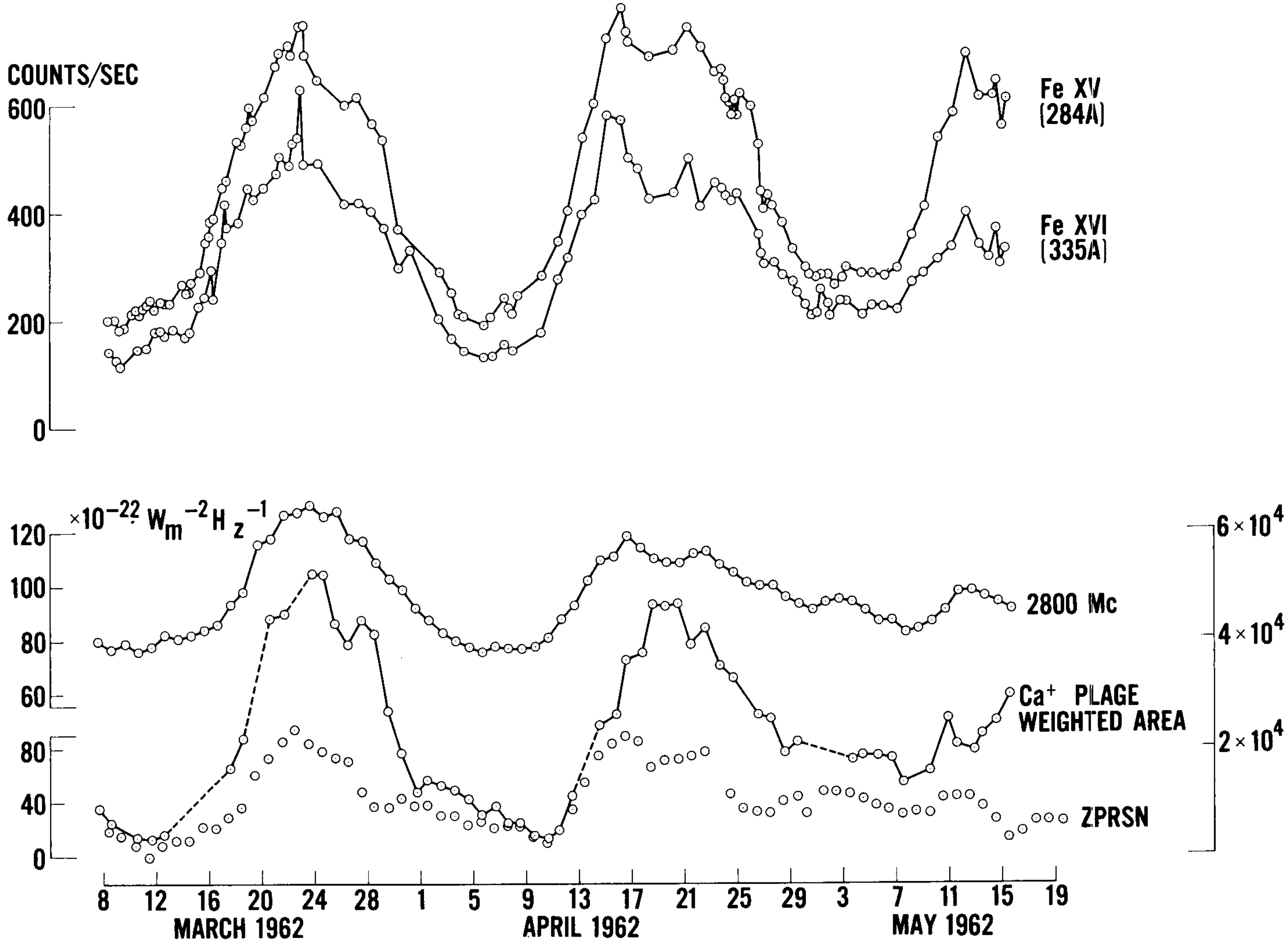

Figure 6 - Fe XV and Fe XVI Lines Compared with Ground-based Measurements of Solar Activity

thus far been observed in the spectral region from 171 A to 400 A; only a few faint lines have smaller non-flare variations than the He II Lyman-alpha line, while no other lines have increases as great as those observed for 284 A and 335 A. A summary of the average increases in counting rates for the period from 9 March to 23 March 1962, a period of increasing solar activity, is given in Table 1. The increase, weighted by the intensity of each line, is computed for the range from 171 A to 305 A, using sixty reliably observed lines. The increase in the range from 305 A to 400 A can only be estimated because of the masking effect of second order images above 342 A. The values given in Table 1 are, of course, appropriate only for the particular interval in time for which they were computed.

TABLE I

INCREASES IN SOLAR EUV SPECTROPHOTOMETER COUNTING RATES

9 March 1962 to 23 March 1962

SPECTRAL RANGE	AVERAGE COUNTING RATE INCREASE
171 A - 228 A	55%
229 A - 300 A	80%
229 A - 305 A	52%
305 A - 400 A	50% (estimated)

The initial analysis of only three lines (He II 304 A, Fe XV 284 A, Fe XVI 335 A) already indicates that the relative prominence of spectral lines may depend upon the age of the center of activity which is responsible for the increased radiation. As an example of this, one may observe (Figure 6) that the maximum emission in the Fe XV apparently occurs later in time than the maximum for the 2800-Mc radio flux or for the plage areas observed during March, April and May. In addition to such a slowly changing effect, one may note that localized perturbations appear (7-9 March and 16-17 April) for which the relative increases are considerably different for the helium and the iron lines. It appears that in these instances we are observing phenomena localized at particular levels in the solar atmosphere.

2. <u>1 - 11 A X-ray Experiment</u>

An experiment to monitor solar X-ray was flown on OSO-1 by W. A. White [6] and R. M. Young of Goddard Space Flight Center. The detector was a beryllium window ion chamber with a Xenon filling. The conversion efficiency as a function of wavelength is shown in Figure 7.

The full-scale sensitivity is dependent upon the shape of the input spectrum. If the spectral shape obtained by Pounds, Willmore, et al [7] from the satellite Ariel, which is consistent with a $2.8(10)^6$ ^oK plasma, is assumed the wavelengths contributing to the output current are in the interval 3-11 A and the full-scale sensitivity is $1.8(10)^{-3}$ ergs cm^{-2} sec^{-1}. For comparison with earlier measurements by R. W. Kreplin, et al [8] over bandwidths specified as 2-8 A, the full-scale sensitivity of the OSO-1 experiment is $3.6(10)^{-4}$ ergs cm^{-2} sec^{-1}.

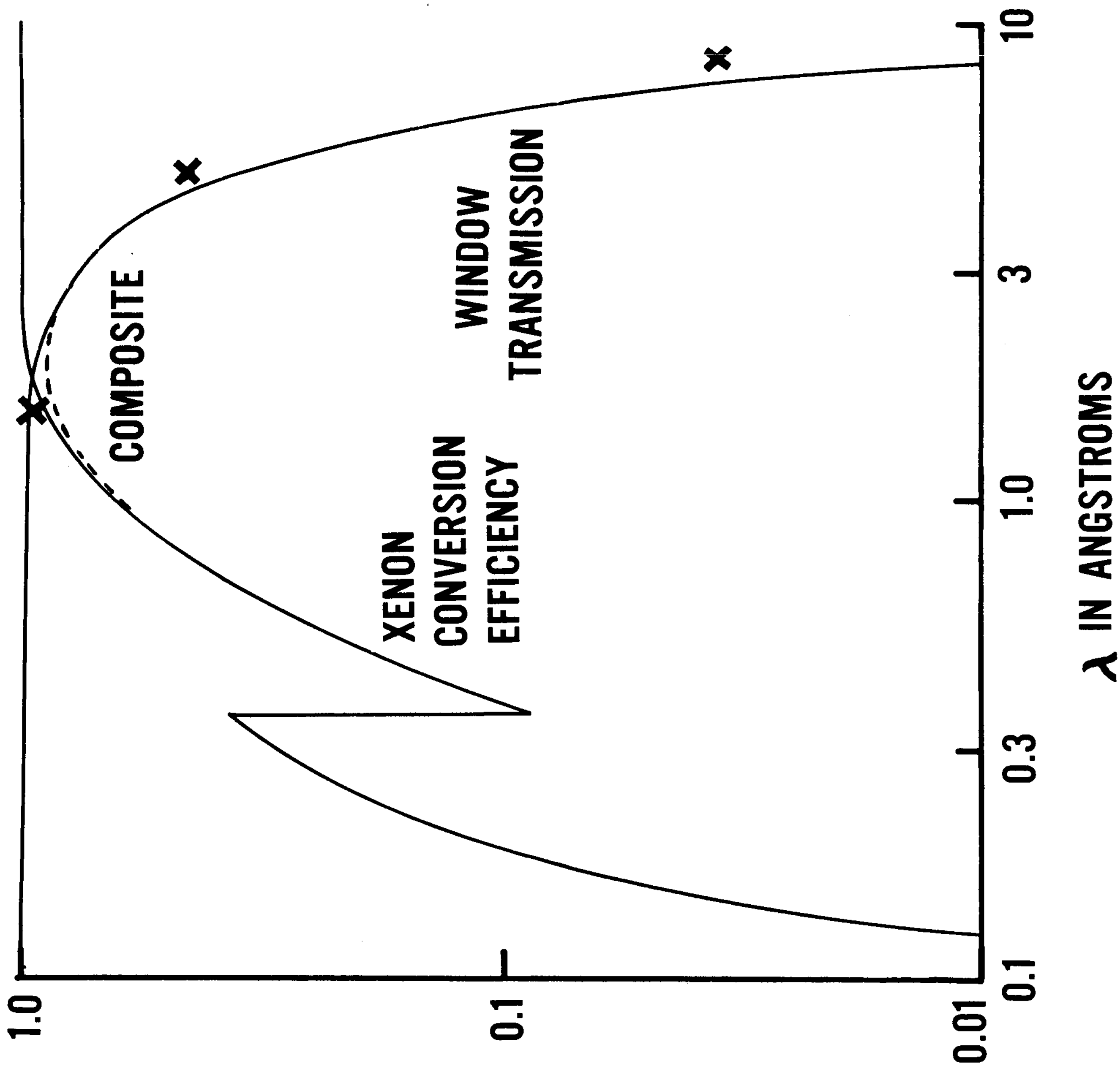

Figure 7 - OSO-1 Ion Chamber Efficiency as a Function of Wavelength

If one computes the continuum flux to be expected at these wavelengths from the entire solar corona, the theoretical flux following the work of Elwert [9] for an isothermal corona with Allen's [10] electron density profile at $2.8(10)^6$ °K falls short of the lowest value measured by OSO-1 by a factor of the order of 15. In fact, the entire corona would have to be at a temperature in excess of $3.5(10)^6$ °K to meet the lowest OSO-1 flux using such an all-continuum model. If one assumes the contribution from line emission in excess of the flux from continuum emission by a factor of 15, the corona in its entirety would have to be at a temperature of about $2.4(10)^6$ °K; to explain the lowest flux measured by OSO-1. For more than 50 percent of the time the OSO-1 flux exceeded this lowest value by at least a factor of 10.

From the fact that most of the time the solar X-ray flux measured by OSO-1 was much larger than the lowest value (which is already uncomfortably high for an isothermal corona with uniform density profile, even with appreciable line emission), we can only conclude that the source of X-rays of less than 11 A wavelengths must conform to localized regions such as plages, as has been observed for longer wavelengths.

A comparison of the slowly-varying part of the 10-Angstrom X-ray flux with 2800-Mc radiation confirms that the localized sources of solar X-rays are associated with centers of activity such as Ca plages and/or sunspot groups. Figure 8 shows the time-history of both fluxes for about 2.5 solar rotations in the early life of OSO-1. It can be seen that the smoothed X-ray flux correlates with the excess 2800-Mc flux above a

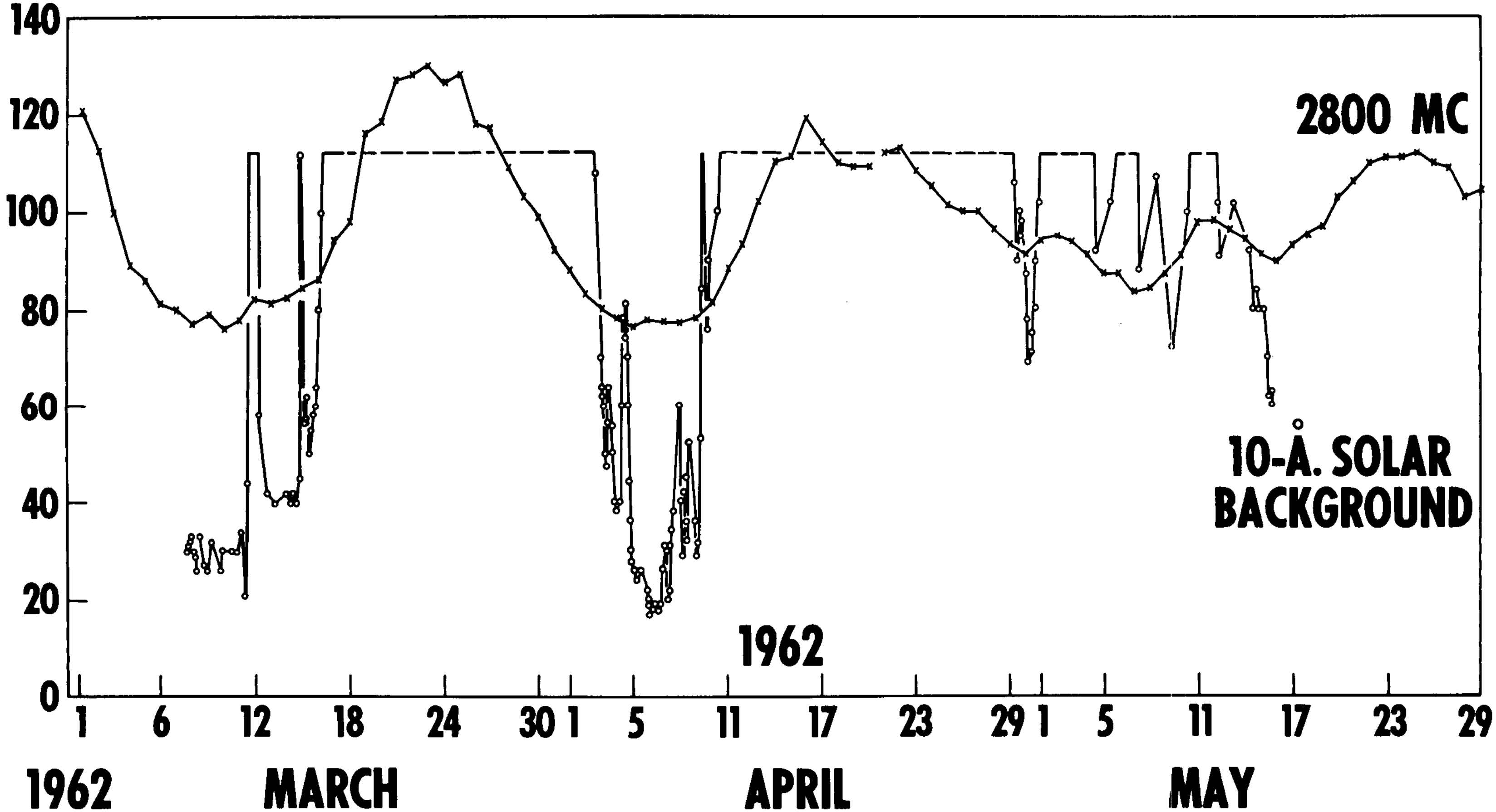

Figure 8 - Slowly-varying Component of Solar X-rays Compared with 2800-Mc Radio Measurements

background of about 75 flux units appropriate for the "quiet" sun at that phase of the solar cycle (Covington and Harvey [11]).

The lowest X-ray flux measured by OSO-1 (April 6, 1962) was: for $\lambda < 8$ A, $3.6(10)^{-5}$ erg cm^{-2} sec^{-1}; for $\lambda < 11$ A, $1.8(10)^{-4}$ ergs cm^{-2} sec^{-1}. This may be considered an upper bound on the X-ray flux from the "quiet" sun. This flux occurred at a time when only 3 plages of area $\geq$ 1000 millionths of a solar hemisphere were visible on the disk. The nearest plage behind the west limb had set three days previously, and the nearest behind the east limb was not to rise until 1.5 days later. If we assume that the X-ray emission is coming from 3 "pillbox" volumes, one associated with each of the 3 plages, each having its base area equal to the plage area and furthermore having a height equal to 1/2 the diameter of its base, the source volume is 3.85×10^{29} cm^3. The volume above one of the plages, #6379, was observed by Billings [12] on 9 April 1962, to have a faint continuum enhancement from which he estimated the electron density $n_e = 0.5(10)^{10}$. Using this as the electron density, and assuming,(as is most likely from such a weak source, Hallam and Young [13]) the electron temperature was not greater than $3.0(10)^6$ ^oK, one finds that in order to obtain the X-ray flux measured on OSO-1 the ratio of line emission to continuum emission must be at least 10:1*. If T_e was no greater than the $2.8(10)^6$ - degree value obtained from the Ariel spectrum of April 27, the ratio of line emission to continuum emission must have been around 30:1.

* A similar conclusion has been suggested by Pounds, Wilmore, Brown, Norman and Sanford [7] based upon the Ariel data.

Up to now we have discussed only the slowly-varying component of the X-ray emission: in addition to these quasi steady-state conditions, transient events (X-ray flares) lasting usually from 10 minutes to a couple of hours were frequently observed. Such an event is shown in Figure 9, and should be compared with the quiet period of similar duration shown in Figure 10. The particular event of Figure 3 contains a total energy below 11 Å of approximately $2(10)^{27}$ ergs.

During the 9-day interval between launch and March 16, 1962 (at which time the rising of plage #6370 on the east limb supplied enough X-ray emission to carry the experiment off-scale), approximately 60 X-ray flare events lasting from 10 minutes to 1 hour were seen, and 4 events were seen to last about 5 hours.

During this same interval (1620 UT March 7, 1962, to 1620 UT March 16, 1962) some 33 H-α flares were reported by ground-based observatories. Of these H-α flares, 6 would have been unobservable from OSO-1 for various reasons (satellite night, failure to command data storage readout, etc.). Of the remaining 27 H-α flares, 3 occurred while the X-ray experiment was still off-scale because of a previous large event. This leaves 24 H-α flares which can be tested for correlation with the X-ray flares. Of this group of 24, it appears that 11 correlate well, 3 definitely have no counterpart in X-rays, and the remaining 10 are doubtful because of insufficient data or an excessive time difference ($>$10 minutes). Conversely, there are 6 full-scale or greater X-ray events for which no H-α flare was reported even though observations were presumably being

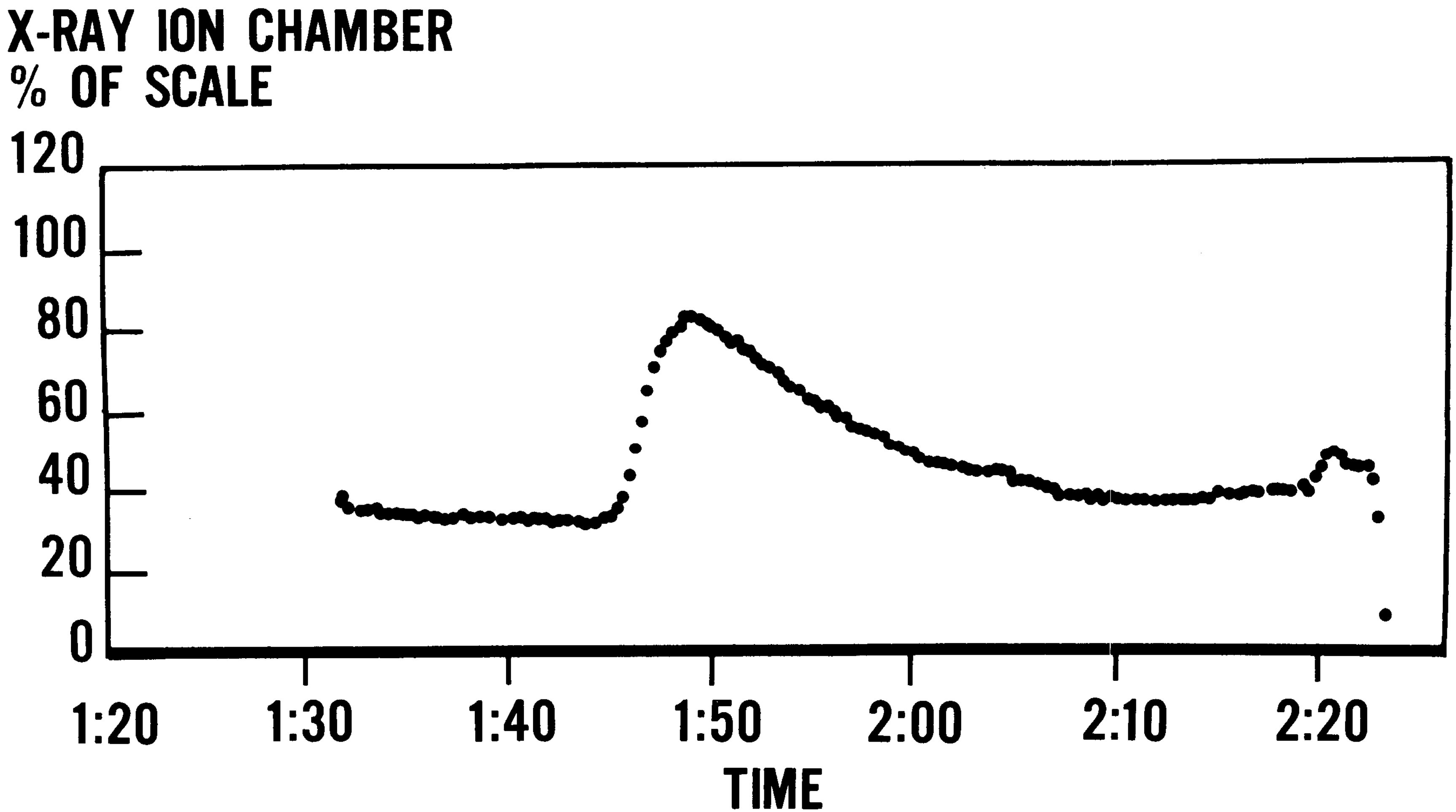

Figure 9 - Small X-ray Flares

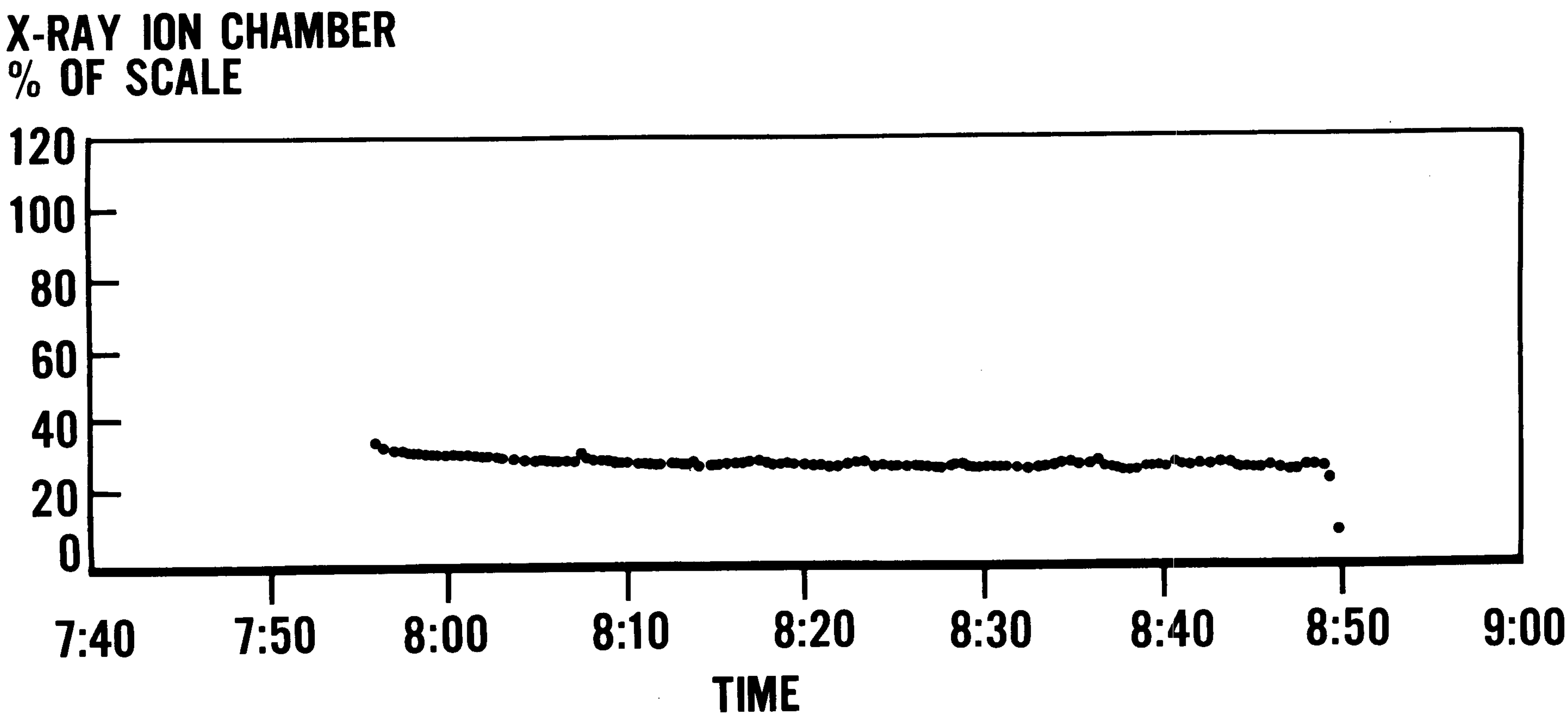

Figure 10 - Typical "Quiet" X-ray Period

made at the time. Certainly more observations will be required before a definite statement can be made regarding a correlation or lack thereof between H-α flares and X-ray flares.

In looking for correlations with Sudden Ionospheric Disturbances, all X-ray events exceeding the full-scale saturation level were barely detectable (if observing conditions permitted) in Sudden Phase Anomaly data for VLF transmissions via the D layer. Only the large event of 13 March was seen in ionospheric indices other than SPA's. Correlation with transients in the 2800-Mc solar flux is good; but again, full-scale X-ray events are represented by extremely small events (1 to 2 flux units) in the 2800-Mc data.

Several apparent associations of certain X-ray flares into groups displaying a definite pattern were observed (White [6]). Figure 5 shows such a grouping. Similar groupings are present in the data for the first week in April; in fact, the one particular March group shown in Figure 11 has an exact April counterpart 27.1 days later, with identical time-separations between events and with identical peak excursions above mean background level. The envelope joining the peaks of the flares within a group is found:

(a) to be a straight line, and

(b) to have the same slope (with either positive or negative sign) from group to group.

These characteristics of the flare groups indicate a constant time rate-of-change of X-ray source strength. Source strength is a function

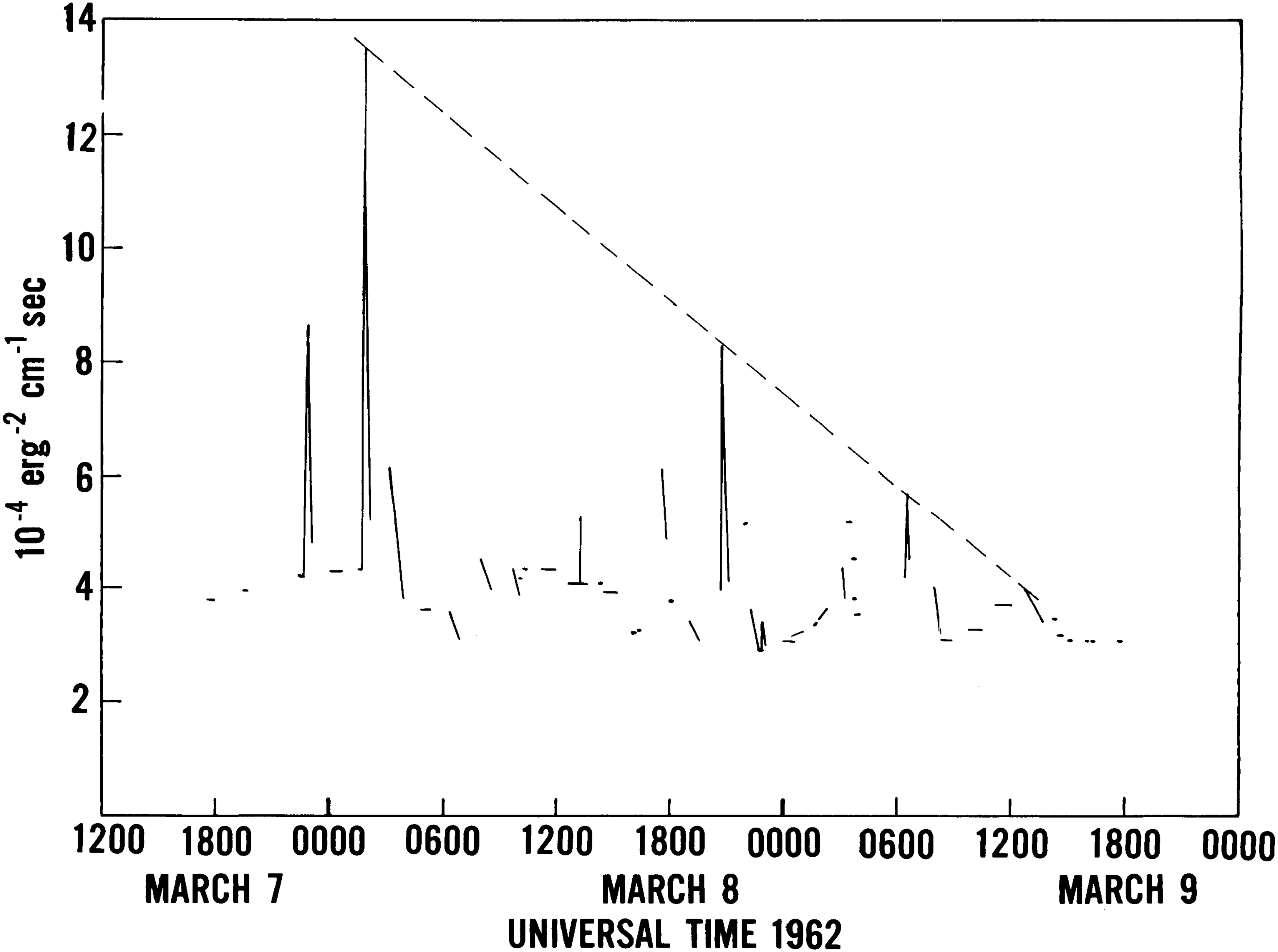

Figure 11 - Grouping of X-ray Flares for Period Marcy 7 - March 9, 1962

of electron density, of temperature, and of volume. It is difficult to see why any time-variation of either electron density or temperature would be of such a particular non-linear natúre as to constrain the source strength to vary linearly with time. One is left with the concept of a volume which is either growing or diminishing at a constant rate, and which on occasion serves as a reservoir of high-temperature electrons and ions interacting to produce the X-ray flares.

3. Hydrogen Lyman-alpha Measurements

The solar hydrogen Lyman-alpha flux was monitored from OSO-1 with an experiment performed by Kenneth Hallam and Robert Young [13] of the Goddard Space Flight Center. The detector used was a CS_2-filled ion chamber with a L_iF window.

The average solar flux measured in the spectral region 1050 A to 1230 A was 4.9 $\pm$ .1 ergs/cm^2- sec. for the first 40 orbits. Lyman-alpha contributes about 95 percent of the flux in this bandpass. The remainder is mainly due to Si III, λ 1206.5 A. After the first 230 orbits, the ion chamber sensitivity declined at about 20 percent per week. This, however, had no effect on short term relative measurements.

A flare of importance 2+ on 13 March caused a peak enhancement in Lyman-alpha of 5.3 percent. An increase of 6.8 percent was observed during an importance 3 flare on 22 March. This represents a local brightening in Lyman-alpha of between 5 and 150 times, depending on the background situation.

4. 20 Kev - 1 Mev Gamma-ray Experiments

Two experiments to search for solar gamma-radiation in the 20 Kev to 1 Mev region were flown by K. J. Frost, E. D. Rothe, K. L. Hallam, W. A. White and H. M. Horstman [14] of the Goddard Space Flight Center. The first experiment consisted of a thin NaI(Tl) crystal (2.22 cm diameter x 0.15 cm height) scintillation counter surrounded by a copper shield. The objective of this experiment was to search for solar bremsstrahlung bursts in the 20 to 100 Kev range. The second experiment consisted of three scintillation counter detectors. Two NaI(Tl) (3.8 cm diameter x 3.8 cm height) crystals were placed in the wheel section of the Observatory and one (3.8 cm diameter x 5.08 cm height) CsI(Tl) crystal was placed in the pointed section. These crystals measured the spectrum of gamma-rays between 0.100 and 1.00 Mev with particular emphasis on the 0.511-Mev positron-electron annihilation line and its temporal variation.

The results of the 20-100 Kev experiment indicate that the flux from the quiet sun cannot be in excess of 3.40 $\pm$ 0.95 photons/cm^2-sec in this energy range. At this time no solar bremsstrahlung bursts have been detected. The data survey thus far includes most of the information acquired during the months of March and April 1962. It is pertinent to note that no solar proton events occurred during this period, at the time observations were being made. The counting rate in the 0.1 to 1 Mev range was found to be 4.7 $\pm$ 0.5 counts/cm^2-sec. The data also indicate that the upper limit of the positron-electron annihilation radiation flux from the sun is 0.6 $\pm$ 0.2 photons/cm^2-sec.

Another gamma-ray experiment was flown by Laurence E. Peterson [15], University of California, La Jolla, California. His experiment was designed to search for extra terrestrial gamma-rays in the 50 Kev - 3 Mev energy range. The apparatus consisted of a 2.5 cm diameter x 1.25 cm height NaI counter with a 0.5 cm lead collimating shield for 50-150 Kev photons. A Compton telescope, consisting of a 3.2 x 3.2 cm NaI counter in coincidence with a phoswich type NaI counter (5.1 cm diameter x 5.7 cm height) provided a directional detector for gamma-rays between 0.3 and 3.0 Mev. The counting rate of the low energy telescope near 0 geomagnetic latitude was 1.0 ± 0.1 counts/cm^2-sec, most of which was local cosmic-ray produced background. The solar flux at the earth was less than 1 photon/cm^2-sec or 1.6×10^{-7} ergs/cm^2-sec between 50 and 150 Kev. No increases were noted during the flares on 11 March and 22 March 1962, and no significant variations above background over the celestial sphere have been observed. Typical total rates measured by the phoswich NaI counter at 0 geomagnetic latitude were 0.40 and 0.18 counts/cm^2-sec for photons with energy losses of 0.3 - 1.0 and 1.0 - 3.0 Mev, and 0.35 counts/cm^2-sec for particles losing more than 1 Mev. The respective rates at 40° geomagnetic latitude were 0.64, 0.44 and 1.6 counts/cm^2-sec. Most of the gamma-rays in this energy region, immediately above the earth's surface, were either due to earth albedo or were of local origin.

5. Proton-Electron Experiment

A proton-electron analyser was flown on OSO-1 by Carlton D. Schrader, Aerospace Corporation, and R. C. Kaifer, J. A. Waggoner, J. H. Zenger and S. D. Bloom [16] of the University of California, Lawrence Radiation

Laboratory. The objective of the experiment was to determine the time and position variations of the fluxes of protons of energies greater than 1.5 Mev and electrons of energies greater than 110 Kev near the lower boundary of the inner Van Allen belt. The detector utilized the principle that in certain scintillators protons and electrons produce fluorescent pulses of distinctly different decay times. This made it possible, through electronic pulse shape discrimination, to employ a single crystal on a single photomultiplier to detect and separately count both protons and electrons.

One of the most interesting preliminary results was the discovery of a number of "warm spots"(as contrasted to the anomalous South Atlantic radiation "hot spot") where the electron flux is more intense, by factors up to 50, than the average intensity. These warm spots are apparently constant in time, intensity and position. They are all located between latitudes 33°N and 33°S (the limiting orbital latitudes of the satellite) and occur over Madagascar, Western Australia, Eastern Australia, northwest of Hawaii, off lower California and in the South Pacific. Preliminary analysis has included the plotting of the warm spot intensities as a function of the natural trapped particle coordinates, B and L. The warm spot intensity plots form well defined curves in B-L space, which differ, however, from curves for similar B and L plotted from data recorded over other geographical locations. Thus, instead of a previously supposed longitudinal invariance, these data seem to indicate that at this altitude (near 575 km) there is a definite dependence on longitude. The experimenters are attempting, in a preliminary theoretical interpretation, to explain the warm spots as being due to trapped radiation which is being supplied at equilibrium rates from the lower Van Allen zone. As these low-altitude trapped electrons drift eastward across the Americas and the Atlantic they are lost because of the South Atlantic anomaly which causes them to mirrow below sea level. This accounts for the low intensities for a given B and L in this region. Even though most of the electrons have just been wiped out in their passage across the Atlantic, warm spots are already re-established just east of Africa. This is regarded as evidence that the warm spots are being constantly supplied from higher altitudes.

The general proton data exhibited less structure, but an apparent small monotonic increase of proton intensity as a function of time is being investigated. To check this point further, it is planned to continue to record additional data (available from the satellite on a real time basis until July 1962). Only one very low intensity proton warm spot has been observed so far, and this is above the Indian Ocean, between Africa and Australia.

Also of considerable interest were the many narrow, but intense, peaks of both protons and electrons which frequently occurred superimposed on the "normal" structure, presumed to be due to precipitation of previously trapped particles by magnetic disturbances. Many such intense peaks were found, e.g., in the data of March 12, 13 and 14, 1962, a period of unusual solar activity. The artificial radiation belt formed by the Starfish high altitude nuclear test (July 9, 1962) was also observed over a limited area and the subsequent time history recorded.

6. <u>High Energy Gamma-Ray Experiment</u>

The high energy gamma-ray detector aboard the OSO-1 was designed by G. G. Fazio [17] of the University of Rochester and the Smithsonian Astrophysical Observatory to provide the first view of a solar flare in the > 100 Mev region of the electromagnetic spectrum. A partial analysis of the data has shown no evidence for this radiation from the sun, even during the importance 3 flare of March 22, 1962, and the importance 2+ flare of March 13, 1962. The upper limit of the flux from each of these flares was estimated to be 10^{-2} photons/cm^2-sec, and that for the quiet sun, 7 x 10^{-3} photons/cm^2-sec. The flux from the total sky was less than 6 x 10^{-3} photons per/cm^2-sec steradian. Locally produced background radiation limited the sensitivity of the detectors. A more complete understanding of this background radiation will permit a sensitivity of 10^{-3} photons per cm^2 per sec from the sun.

7. <u>Solar Neutron Experiment</u>

An experiment to detect solar neutrons was flown on OSO-1 by W. H. Hess [18], of the University of California, Lawrence Radiation Laboratory and Goddard Space Flight Center. The detector was a $B^{10}F_3$ proportional counter and the purpose was to observe diurnal variations of its counting rate, as well as the Hames sunset effect. Combining data from 42 orbits gave essentially no pre-sunset maximum to within 10 percent. However, there appeared to be a variation of the neutron count rate from day to night. The preliminary ratio of count rates day/night is 1.08 ± .01. It is currently uncertain whether there is associated with this daytime neutron excess a concurrent proton excess.

SUMMARY OF OSO-1 OBSERVATIONS

Observations of the sun were made by OSO-1 for a time period corresponding to approximately three solar rotations on almost continuous basis and on a real time over the ground stations basis for approximately one year. The results reported here were based upon partial analysis of the first three months data.

The observations of the solar spectrum between 170 A and 340 A have shown:

1. That the He II (304 A) emission is enhanced by a factor of about 33% during a period when the Zurich Provisional Relative Sunspot Number increased from zero to a maximum of 94 and the 2800-Mc flux varied from approximately 76 to 125 x $10^{-22} wm^{-2} Hz^{-1}$.

2. The Fe XV (284 A) and Fe XVI (335A) coronal lines were enhanced during the same period by a factor of approximately four.

3. The enhancement of He II (304 A) and Fe XV (284 A) and Fe XVI (335 A) due to plage activity was larger than enhancements due to flares that occurred during the three-month interval of the observations.

4. The variations in intensity of the He II (304 A), Fe XV (284 A) and Fe XVI (335 A) represent the extremes observed. If one averages sixty of the reliably observed lines between 171 A and 342 A the enhancement is between 50% and 80% for the time interval 9 March to 23 March.

5. Although there appears to be a gross correlation between solar activity indices (such as 2800-Mc flux) and the He II, Fe XV and Fe XVI fluxes, there are indications that the relative prominence of the spectral lines may depend upon the age of the center of activity.

The 1 - 11 A X-ray measurements have observed a slowly-varying component which correlates with the slowly-varying component of the 2800-Mc solar radiation. A model for these quasi-stable X-ray sources which fits the OSO-1 data postulates localized sources having the same horizontal extent as Ca plages with thicknesses proportional to their diameter, and having an electron temperature of $2.8(10)^6$ °K or greater and an electron density of about $5(10)^9$ electrons per cm^3. For these conditions it is also necessary that the ratio of line emission to continuum emission be at least 10:1 and more probably 30:1.

In addition to a slowly-varying component, transient events (X-ray flares) lasting from 10 minutes to a few hours were frequently observed. Correlation has been attempted with H-α flares with somewhat ambiguous results. X-ray flares were frequently observed to be associated in groups possessing a characteristic pattern; the concept of a source volume varying linearly with time is suggested to account for the linear envelope of a flare group.

The average hydrogen Lyman-alpha flux was approximately 4.9 ergs/cm^2-sec and for the first time an enhancement of Lyman-alpha has been observed during solar flares. The enhancement was 5.3 percent during a class 2+

flare and 6.8 percent during a rather unusual class 3 flare (practically no geophysical effects were observed for this flare).

No solar bremsstrahlung X-ray bursts (10-100 Kev) have been found in the data examined to date. An upper limit for "quiet" sun X-rays of this energy range was found to be 3.40 ± 0.95 photons/cm^2-sec. For 50-150 Kev X-rays the upper limit found was 1 photon/cm^2-sec. No gamma-rays $>$ 100 Kev have been observed.

The proton-electron experiment discovered a number of "warm spots" below the normal inner belt. These radiation "warm spots" apparently were constant in time, intensity, and position. They were found over Madagascar, Western Australia, Eastern Australia, Northwest of Hawaii, off lower California and in the South Pacific.

To date no high energy gamma-rays (Energies $>$ 100 Mev) have been detected from the sun either during a "quiet" sun or a solar flare.

The solar neutron experiment has detected a very slight excess in neutron count from day to night, $1.08 \pm .01$. It is currently uncertain whether this excess is real and whether there is a corresponding proton excess.

CAPTIONS

Figure 1	-	OSO-1 Spacecraft
Figure 2	-	Slip Ring Performance
Figure 3	-	Typical Solar Spectrum 170 A - 400 A
Figure 4	-	Comparison of Two Spectra Representing "Quiet" and "Active" Sun
Figure 5	-	He II Lyman-alpha Line Compared with Ground-based Measurements of Solar Activity
Figure 6	-	Fe XV and Fe XVI Lines Compared with Ground-based Measurements of Solar Activity
Figure 7	-	OSO-1 Ion Chamber Efficiency as a Function of Wavelength
Figure 8	-	Slowly-varying Component of Solar X-rays Compared with 2800-Mc Radio Measurements
Figure 9	-	Small X-ray Flares
Figure 10	-	Typical "Quiet" X-ray Period
Figure 11	-	Grouping of X-ray Flares for Period March 7 - March 9, 1962

REFERENCES

1. F. P. Dolder, O. E. Bartoe, R. C. Mercure, Jr., R. H. Gablehouse, and J. C. Lindsay, (1963) Space Research III, COSPAR, Preiester Ed., North Holland Publishing Co.

2. W. E. Behring, W. M. Neupert and J. C. Lindsay, (1963) Space Research III, COSPAR, Preiester Ed., North Holland Publishing Co.

3. H. Zirin, L. A. Hall and H. E. Hinteregger, (1963) Space Research III, Preiester Ed., North Holland Publishing Co.

4. W. M. Neupert and W. E. Behring, J. Quant. Spectrosc. Radiat. Transfer. Vol. 2, 527 (1962).

5. W. M. Neupert, W. E. Behring and J. C. Lindsay, Space Research IV (To be published) 1964.

6. W. A. White, Space Research IV (To be published) 1964.

7. K. A. Pounds, A. P. Willmore, P. J. Bowen, K. Norman and P. W. Sanford; Proc. Roy. Soc. (In Press).

8. R. W. Kreplin, T. A. Chubb, H. Friedman; Jour. Geophys. Res. 67 (1962) 2231.

9. G. Elwert, Jour. Geophys. Res. 66 (1961)391.

10. C. W. Allen, Monthly Notices Roy. Astr. Soc. 106 (1946) 22.

11. A. E. Covington and G. A. Harvey, Astrophys. Jour. 132.

12. D. E. Billings, Private Communication

13. K. L. Hallam and R. Young, Presented at Spring meeting of AGU, April 1963.

14. K. J. Frost, E. D. Rothe, K. L. Hallam and W. A. White, H. M. Horstman, Presented at Spring Meeting of AGU(April 1963).

15. L. E. Peterson, Presented at Spring Meeting of AGU, April 1963.

16. C. D. Schrader, R. C. Kaifer, J. A. Waggoner, J. H. Zenger and S. D. Bloom, Presented at Spring Meeting of AGU, April 1963.

17. G. G. Fazio, Presented at Spring Meeting of AGU, April 1963.

18. W. H. Hess, Presented at Spring Meeting of AGU, April 1963.